nature climate change

SUPPLEMENTARY INFORMATION

DOI: 10.1038/NCLIMATE2574

S1 Ice-Core Data

S1.1 Ice-core temperature and accumulation rate histories and uncertainties

EDC, EDML, Talos Dome, and Vostok records

Temperature histories were derived by Stenni et al.[1] for the EDC and EDML isotope records and by Petit et al.[2] for the Vostok record; each record had been corrected for changes in mean ocean isotopic composition. For Talos Dome, we corrected the ice-core $\delta^{18}O$ record for changes in mean ocean isotopic composition[3], and derived the temperature history based on the isotope/temperature scaling from Stenni et al.[4].

We use accumulation-rate (AR) histories derived by Veres et al.[5] for these four ice cores based on an improved version of the Datice methodology developed by Lemieux-Dudon et al.[6]. Each AR history was initially reconstructed based on the classical empirical relationships with isotopic content[7], which links the precipitation rate to the inversion temperature, the inversion temperature to the mean annual temperature, and then the mean annual temperature to the isotopic content of ice. We call this the $AR_{temperature}$ reconstruction. Several approaches derived from these relationships have been applied, including using an exponential relationship with the isotopic (deuterium or oxygen) content of the ice (which is a proxy for temperature based on the spatial slope of the present-day isotopic thermometer and following correction for variations in the isotopic composition of the mean ocean), using the saturation vapor pressure, or using a linear relationship between the surface temperature and the temperature when and where snow formed (condensation temperature). Parennin et al.[8] note, however, that all formulations give the same results (within 1%) after adjustment of the coefficient that determines the glacial-interglacial amplitude of accumulation changes.

Insofar as this approach is based on the assumption that we are evaluating here, i.e., that there is a reasonably well-defined relation between temperature and accumulation rate, Datice further evaluates this assumption by using an inverse method that generates an optimal compromise between an *a priori* scenario from a glaciological model (that is in part based on the initial $AR_{temperature}$ reconstruction) and the chronological information derived from known-age markers (volcanic ashes, ^{10}Be, ice- and gas-age markers, ice and gas stratigraphic links). In this way, the $AR_{temperature}$ reconstruction assumption is evaluated and adjusted as needed to provide the optimal agreement with the independent age markers.

The first step in this approach is to use an ice-flow model to develop a preliminary age model

DOI: 10.1038/NCLIMATE2574

for the ice core based on the $AR_{temperature}$ and temperature reconstructions[8]. The ice-flow model has two components: the initial annual layer thickness (i.e. the accumulation rate) and the vertical compression of the layers, or total thinning ratio, as evaluated with a mechanical model. The age at a depth z in the ice core is then inversely related to the accumulation rate and temperature.

This ice-flow model contains several poorly known parameters, including the relation between temperature and AR. Accordingly, the parameters are constrained by independent age markers, allowing the model to provide a smooth interpolation of all unconstrained periods.

The second step is a probabilistic inverse approach based on a Bayesian inference developed by Lemieux-Dudon et al.[6], which produces a compromise between the *a priori* modelled glaciological scenario and chronological information given by the age markers. In particular, the method optimizes the accumulation rate, the thinning function and the close-off depth calculated by the direct model in order to obtain a final age scale agreeing with all the age markers. The AR in each ice core calculated by the inverse method still shows a positive relation with temperature, but does differ from the one deduced from the isotopes, with glacial-interglacial amplitude being more pronounced using the inverse method at Talos Dome[9] and less pronounced at EDML[6].

We assume that errors in the temperatures and accumulation rates are independent of each other and thus analyze them separately. We used the $\pm 2^{o}$C uncertainty in glacial-interglacial temperature change reported by Stenni et al.[1] for the EDC and EDML temperature records (Fig. S1 for EDC), and a -10% to +30% uncertainty for the Talos Dome and Vostok temperature records[10]. In the latter case, based on multiple lines of evidence (isotope-enabled GCM simulations under different boundary conditions, deuterium excess information, gas age-ice age differences at times of abrupt changes, inverse modeling of ice-core chronologies), Jouzel et al.[10] concluded that, for a given source region and seasonality, the constraint on interpreting the isotopic profiles at a given core site through time (temporal slope) is within -10 to +30% of the relationship derived for present-day isotopic values and temperature at Antarctic sites spanning some regional scale (spatial slope). This result has since been independently supported by other studies, including those obtained after correction for changes in source conditions from co-isotopic measurements of δD_{ice} and $\delta^{18}O_{ice}$[11,12], and is consistent with the uncertainty derived for the EDC and EDML ice cores by Stenni et al.[1].

Uncertainties on the accumulation rates result from background errors (thinning history, accumulation rates, lock-in depth) and observational errors (age markers). Uncertainties in accumulation rates estimated by Datice increase with time. Average uncertainties range from 6-10% for the Holocene period (0-11 ka), 15-21% for the deglacial period (11-18 ka), and 26-42% for the Last Glacial Maximum period (18-21 ka) (see Figure S1 for EDC).

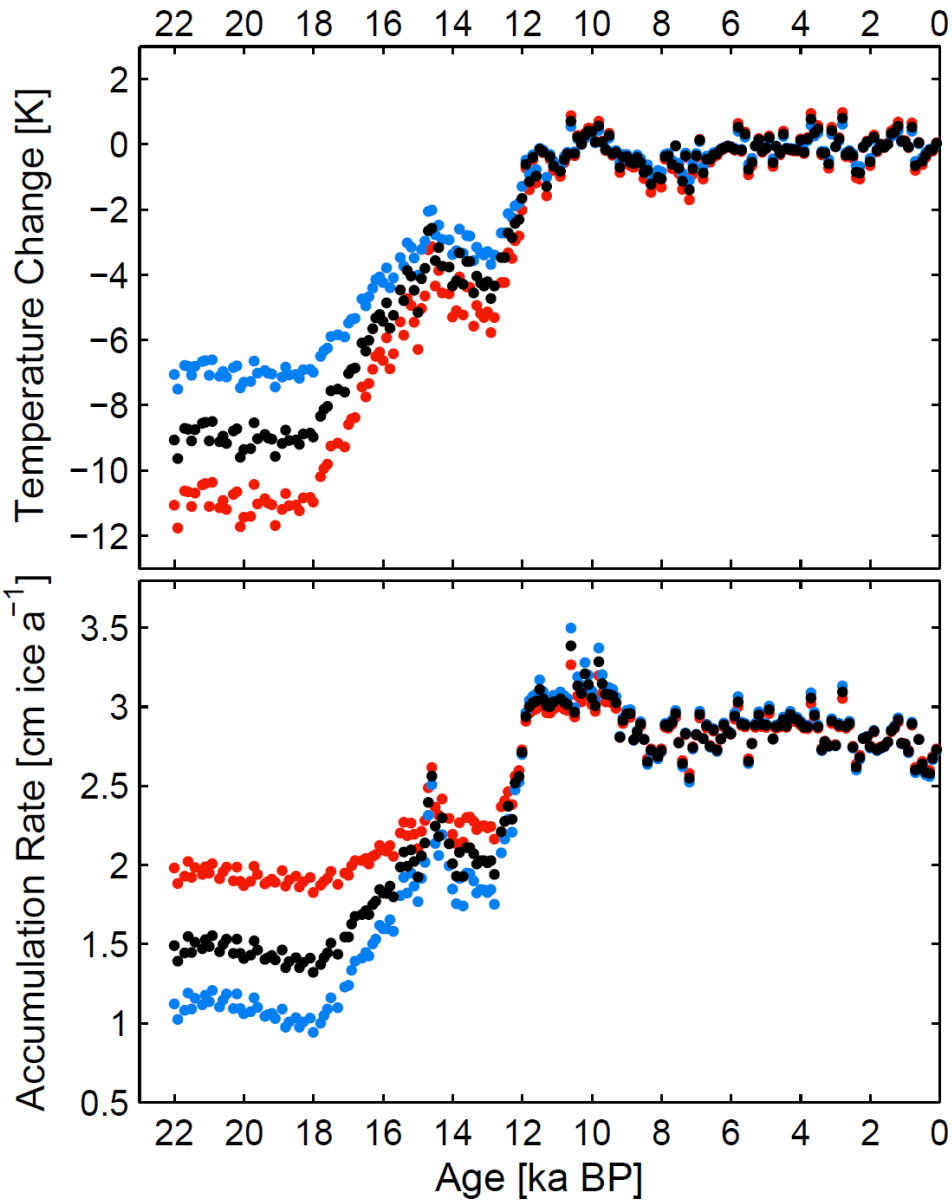

Figure S1: Temperature and accumulation rate scenarios used in assessing the uncertainty in the accumulation sensitivity at EDC (100 year binned data). Scenarios used to estimate a lower bound on the accumulation sensitivity are plotted in red; scenarios used to estimate the upper bound are plotted in blue; the best estimates for T_{site} and AR are shown in black.

Law Dome record

The Law Dome $\delta^{18}O$ record is from Morgan et al. (2002)[13] and Pedro et al. (2011)[14]. We corrected the $\delta^{18}O$ record for changes in sea water[3], and derived the temperature history

DOI: 10.1038/NCLIMATE2574

based on the isotope/temperature scaling of 0.44 ‰ K^{-1} as recommended by van Ommen and Morgan[15].

van Ommen et al.[16] derived the Law Dome AR from age tie-points and an ice-flow model that simulates ice thinning from vertical strain. The first step involves fitting observed layer thinning as a function of depth with a model, and then converting layer thicknesses to meters of ice equivalent by accounting for densities of firn and ice. The age model for the ice core is then based on distinct changes in ice-core properties, such as changes in composition of trapped air, changes in dust concentration, or changes in the isotopic composition of the ice, which can be correlated to changes in other records with known age. van Ommen et al. note that the Law Dome AR during the Holocene is substantially higher than predicted by the AR-$\delta^{18}O$ relationship during the deglaciation[16], which they attribute to increased precipitation from cyclonic systems at this coastal site. Following their assessment, we evaluate the accumulation sensitivity for the 22-9.7 ka interval, during which there is a clear link between AR and temperature. Using the full 22-0 ka interval yields a higher accumulation sensitivity of 7 % K^{-1}.

To investigate the uncertainty in the AR-T slope, we reconstructed minimum and maximum temperature scenarios by using the estimated present-day temporal (0.33 ‰ K^{-1}) and spatial (0.65 ‰ K^{-1}) isotopic sensitivities, respectively, as reported by Morgan et al.[13]. We use the stated uncertainty in the Law Dome AR estimates by van Ommen et al.[16]; during the LGM this is 50-200% of the reconstructed values.

WAIS-Divide record

The West Antarctic Ice Sheet (WAIS)-Divide ice core provides accurate estimates of past AR variability due to the annual layer count going back to 31 ka[17,18]. Moreover, due to the high AR and large ice thickness, the WAIS-Divide core allows for calibrating the water isotope-temperature relationship using the measured borehole temperature profiles as has been done in Greenland[19–21]. Using the preliminary AR and temperature reconstructions and their uncertainties as presented in Buizert et al.[18], we find an AR reduction of 5.5 ± 1.3 % per K of cooling; the uncertainty in the slope is composed of the uncertainty in the temperature reconstruction (5.5 ± 0.7 % K^{-1}) and the uncertainty in the accumulation reconstruction (5.5 ± 1 % K^{-1}).

S1.2 Accumulation sensitivities derived from ice-core data and paleo simulations

For all the ice cores, time series of AR and site temperature (T_{site}) have different temporal resolution. To assess the AR-T_{site} relationship, we have thus binned the data into durations of 100 years for the Vostok, EDC and EDML ice cores and 50 years for Talos Dome and WAIS-Divide ice cores; for Law Dome, we used the irregular interval durations provided in the AR

reconstruction by van Ommen et al.[16]. All data points (either AR or T_{site}) falling within each bin were averaged. For consistency with the CCSM3 simulations, we only evaluate the 22-0 ka interval in the ice-core records, with the exception of the Law Dome ice core, where we evaluate the 22-9.7 ka interval as explained in section S.1.1.

Absolute accumulation data are then plotted against temperature changes, which are given relative to the temperature average of the last 2 ka, except for Law Dome where we express T_{site} relative to 9 ka. To estimate the associated reference level for the accumulation rates (AR_{ref}), a linear trend line is fitted through the data whose intercept (Figure S1) is used as the reference level of accumulation to describe relative changes (Figure 1). The accumulation sensitivity is then estimated via linear regression of T_{site} versus $(AR-AR_{ref})/AR_{ref}$. Note that this latter linear regression fit has intercept of zero, due to the normalization with AR_{ref}.

Accumulation sensitivities from the CCSM3 simulations are calculated in the same way; temperature changes are expressed relative to the average temperature of the last 2 kyr, and the T_{site}=0 intercept of the T_{site}-AR linear fit is used as AR_{ref}. The CCSM3 AR and T_{site} time series have the same temporal resolution (10-year time step), and no binning is required. For comparison to the RACMO data (Figure 2 and 4), the reference period is changed to the present-day period (1890-1980).

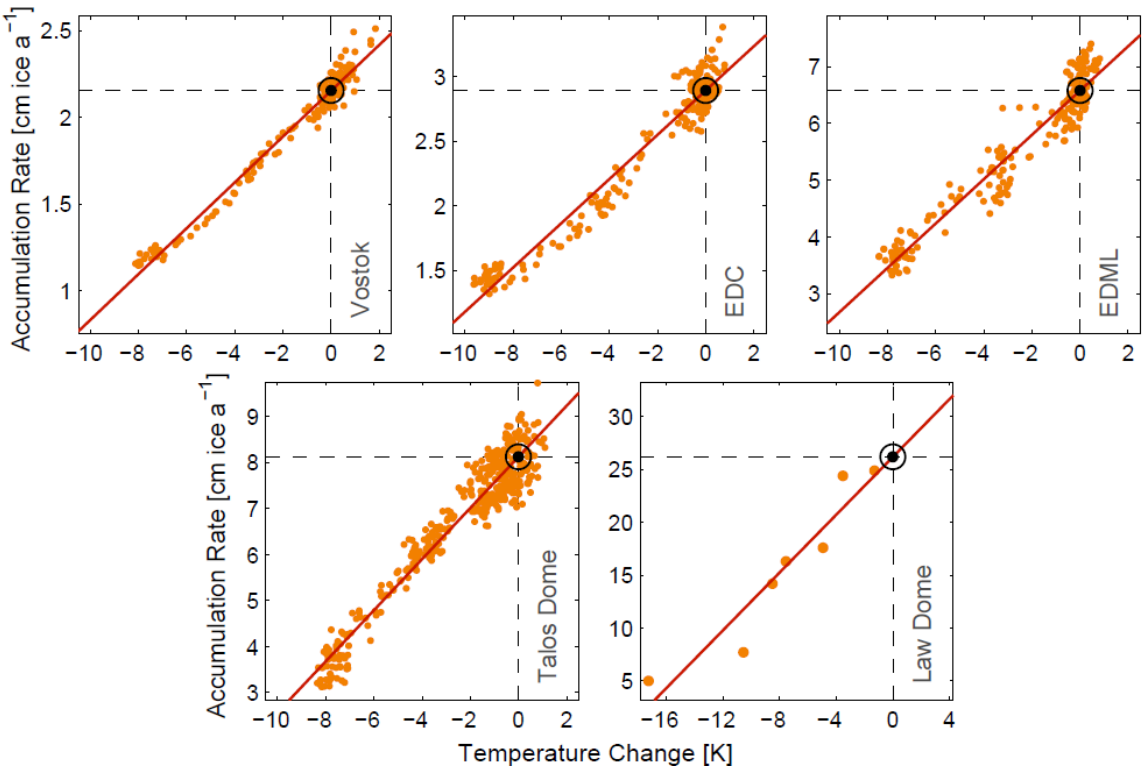

Figure S2: Absolute accumulation rate (in cm yr^{-1} ice equivalent) versus temperature anomaly (relative to last 2-kyr average except for Law Dome, which is for 9 ka) for the ice

DOI: 10.1038/NCLIMATE2574

cores. A linear trend is fitted through these points (red line). The intercept (black dot) is used as the reference level AR_{ref} to describe relative changes in accumulation.

Uncertainty analysis of ice-core accumulation sensitivities

The magnitude of the glacial-interglacial contrast in temperature and accumulation rate determines the slope in the T_{site}-AR scatterplots of Figures 1 and S2. Based on the ice-core uncertainties discussed in Section S1.1, we have constructed alternative AR and T_{site} histories that either minimize or maximize the glacial-interglacial contrast; Figure S1 shows the EDC scenarios as an example.

We derive the uncertainty in the accumulation sensitivity by first accounting for the uncertainty in temperature. We perform the slope-fitting procedure for each of the three temperature scenarios using the best-estimate AR history, which yields three values for the accumulation sensitivity (Figure S3, left panels). We use the standard deviation of the three values as our estimate of the uncertainty in the accumulation sensitivity due to uncertainties in the temperature history. Similarly, the uncertainty of the accumulation sensitivity that accounts for the uncertainty in accumulation rate is calculated by taking the standard deviation of the three slopes associated with the three AR scenarios (Figure S3, right panels). We then add the temperature and accumulation-rate uncertainties in quadrature to derive the total uncertainty for each ice-core record as the square root of this sum. The value is interpreted as the 2σ uncertainty of the sensitivities.

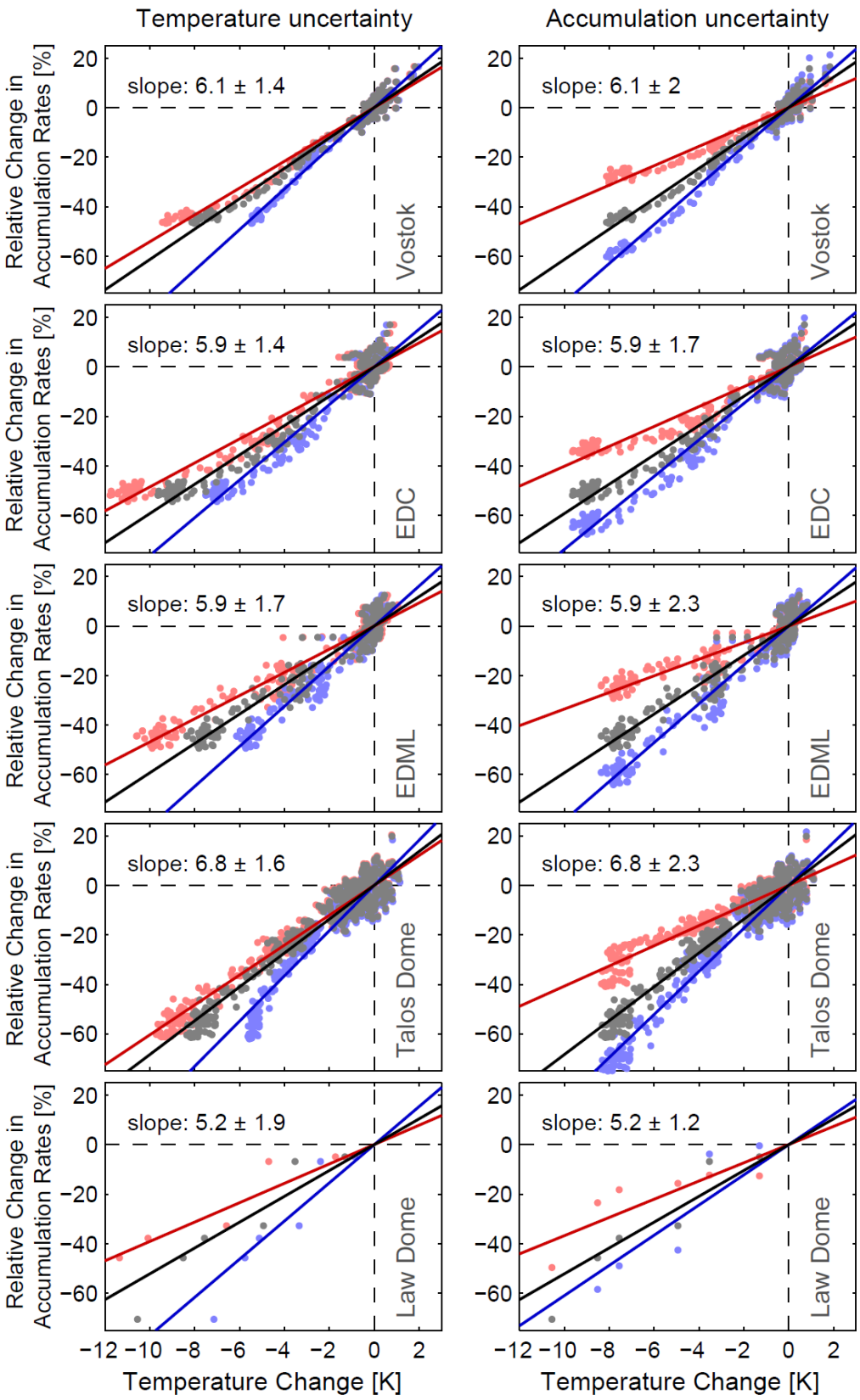

Figure S3: Uncertainty in the accumulation sensitivity for the ice cores due to uncertainty in the temperature reconstructions (left panels) and due to uncertainty in the accumulation

DOI: 10.1038/NCLIMATE2574

reconstructions (right panels). The lower bounds on the accumulation sensitivity are plotted in red; the upper bounds are plotted in blue. The individual temperature and AR contributions to the uncertainty are added in quadrature to obtain the total uncertainty.

S1.3 Elevation changes in the CCSM3 paleo-simulations

During the last deglaciation, mass was lost from the Antarctic and Northern Hemisphere ice sheets. To be consistent with this trend, the CCSM3 paleo-simulations impose several reductions in the Antarctic ice-sheet elevation, the largest of which occurs around 11.3 ka. Lowering the surface elevation induces a simulated warming at the ice coring sites (via the atmospheric lapse rate) that is glaciological rather than climatological in origin. Here we investigate whether the abrupt elevation change at 11.3 ka influences our derived accumulation sensitivity. Figure S4 shows the model output for the full simulation (22-0 ka, blue dots) at the WAIS-Divide site, where the imposed elevation change is largest of the six ice-core sites considered here. We also plot the model output for a 500-year window centered on 11.05-11.55 ka (red dots). Linear fits to both the red and blue data sets have nearly identical slopes (4.5 and 4.4 % K^{-1}, respectively), thus showing that in the CCSM3 simulations, the AR response to climatically and glaciologically induced warmings are the same. To first order, we thus conclude that errors in the CCSM3 surface elevation history should not bias the comparison between ice-core and model-derived accumulation sensitivities.

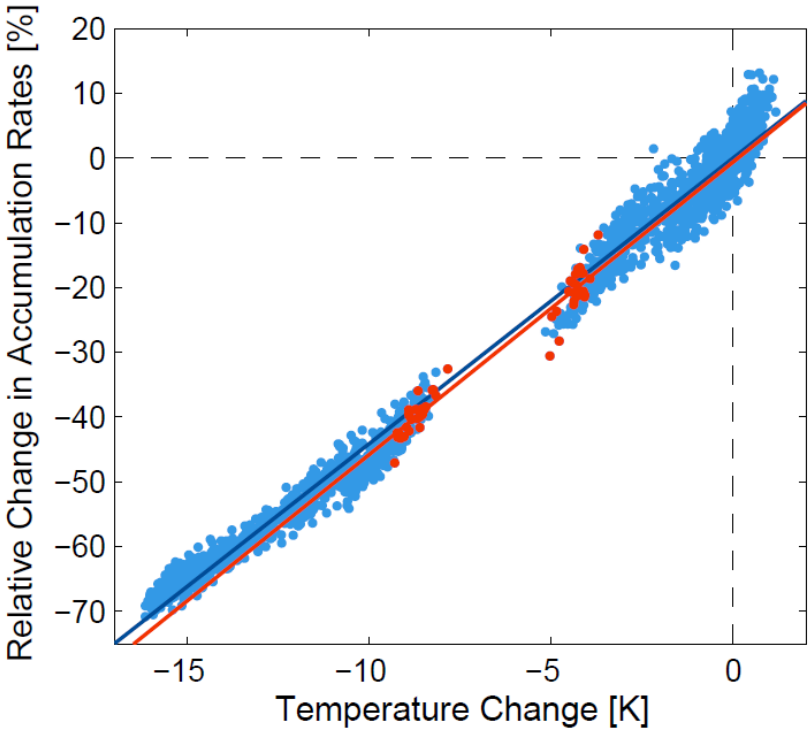

Figure S4: The influence of elevation change on the estimated accumulation sensitivity from the CCSM3 paleo-simulations at the WAIS-Divide site, where imposed elevation changes are largest. Blue dots show the entire 22-0 ka simulation; red dots show model output from a 500-year time window centered around the 11 ka elevation drop. Linear regression gives slopes of 4.4 % K^{-1} and 4.5% K^{-1} for the blue and red data, respectively.

S2 Translation of accumulation changes into sea level change

To estimate the response in sea level changes induced by Antarctic accumulation changes, we did five different simulations with the ice-sheet model PISM. Starting from an equilibrium simulation based on present-day reference accumulation rates, the model was forced by step increases in relative accumulation rates as described by RACMO2 (Fig.4B) associated with a continental warming of 1°C, 2°C, 3°C, 4°C, and 5°C, respectively. After 100 years of constant forcing the associated sea level drop depends almost linearly on the forcing (Fig. S5).

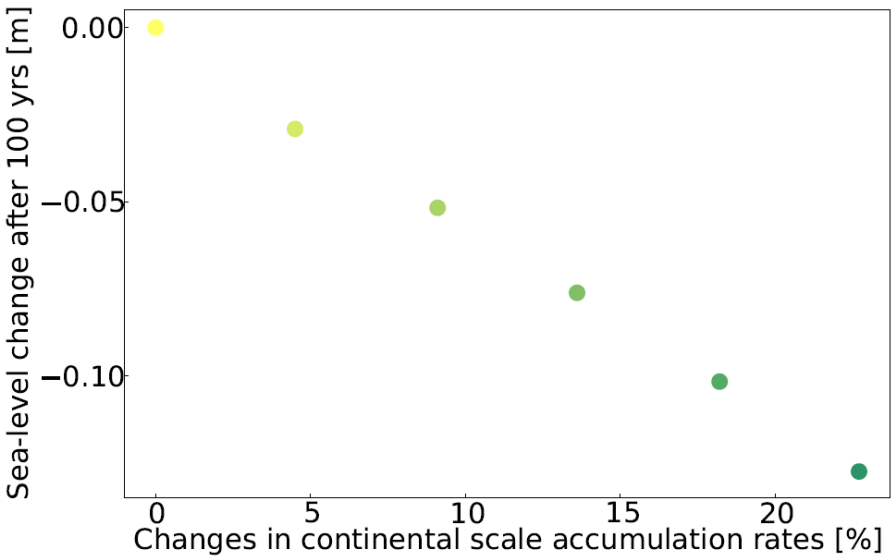

Figure S5: Sea level change after 100 years of constant forcing in terms of the step increase in continental scale accumulation rates at the beginning of the forcing.

We used the five different simulations to estimate the parameters α and γ of a response function

$$R(t) = \gamma * (\frac{t}{t_0})^{\alpha}$$

DOI: 10.1038/NCLIMATE2574

assuming that the temporal evolution of sea level drop can be described as the convolution of response function and the continental-scale relative change in accumulation rates:

$$\Delta M\,(t) \;=\; \int_0^t \Delta A\,(t')R(t-t')dt',$$

We get the best fit for the five different experiments for γ = 7.95 mm yr^{-1} and α = -0.1 (Fig S6). In a sensitivity study, we also used uniform step increases of accumulation rates of 5, 10, 15, 20, and 25% and derived similar parameter values of γ = 6.67 mm yr^{-1} and α = -0.1. The associated response function provides a similarly good fit to the sea level changes simulated for the original step increases based on the RACMO2 pattern (Fig. S6). Thus, the response does not seem to be very sensitive to the actual spatial pattern of the forcing.

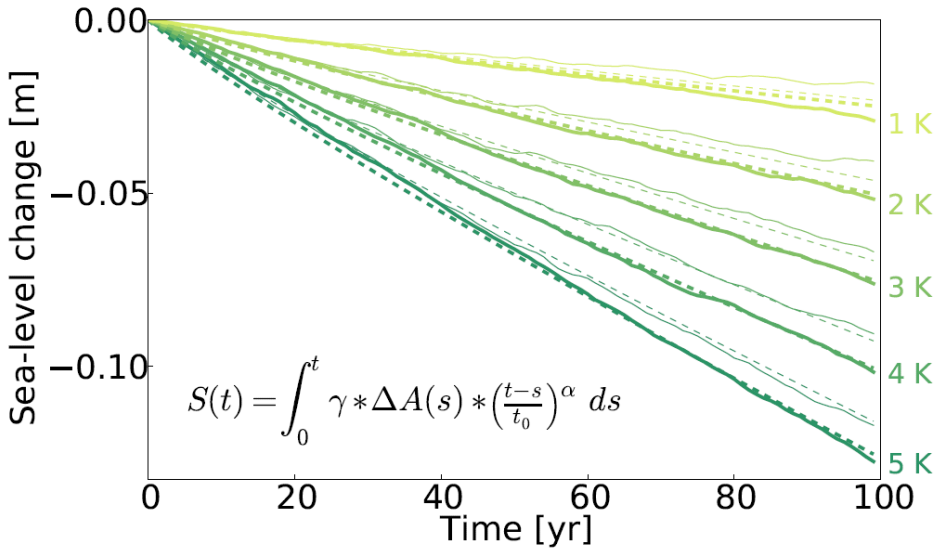

Figure S6: Responses to step increases of accumulation rates corresponding to a continental scale warming of 1, 2, 3, 4, and 5K, respectively. Thick solid lines: PISM simulations based on a step increase of accumulation following the RACMO2 pattern. Thick dashed lines: Reproduction based on the associated response function. Thin dashed line: Reproduction of the PISM simulations based on the RACMO2 pattern of changes by the response function derived from the step increase in forcing assuming a uniform increase in accumulation. Thin solid lines: PISM simulations based on a uniform step increase in relative accumulation changes.

Both response functions also provide a very good fit to a PISM simulation forced by the accumulation changes provided by RACMO2 for the SRES1AB scenario that was used to calculate the accumulation sensitivities (see Fig. S7).

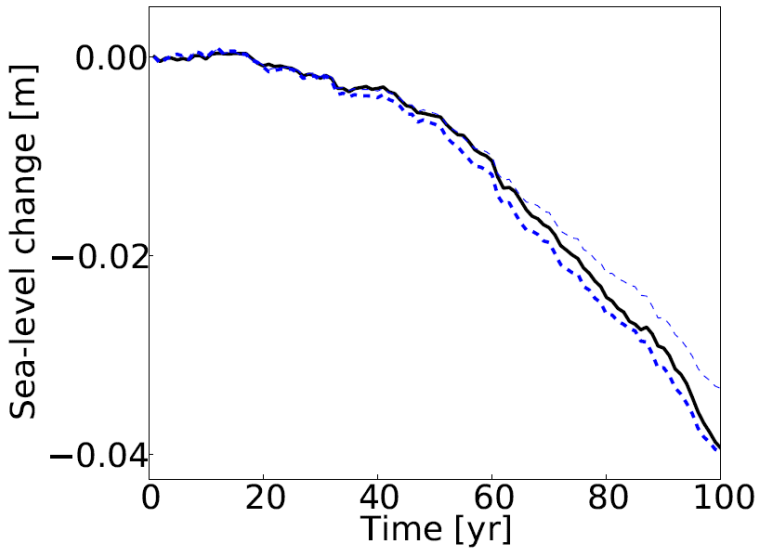

Figure S7: Snow fall induced changes in sea level based on accumulation changes provided by RACMO2 for the SRES1AB scenario. Solid black: Simulations by the ice sheet model PISM. Thick dashed blue line: Reproduction based on the response function derived from the RACMO2 pattern of relative changes. Thin dashed blue line: Reproduction based on the response function derived from a uniform pattern of relative changes.

References

1. Stenni, B. *et al.* The deuterium excess records of EPICA Dome C and Dronning Maud Land ice cores (East Antarctica). *Quat. Sci. Rev.* **29,** 146–159 (2010).

2. Petit, J. R. *et al.* Climate and atmospheric history of the past 420,000 years from the Vostok ice core. *Nature* **399,** 429–436 (1999).

3. Waelbroeck, C. *et al.* Sea-level and deep water temperature changes derived from benthic foraminifera isotopic records. *Quat. Sci . Rev.* **21,** 295–305 (2002).

4. Stenni, B. *et al.* Snow accumulation rates in northern Victoria Land, Antarctica, by firn-core analysis. *J. Glaciol.* **46,** 541–552 (2000).

5. Veres, D. *et al.* The Antarctic ice core chronology (AICC2012): an optimized multi-parameter and multi-site dating approach for the last 120 thousand years. *Clim. Past* **9,** 1733–1748 (2013).

6. Lemieux-Dudon, B. *et al.* Consistent dating for Antarctic and Greenland ice cores. *Quat. Sci. Rev.* **29,** 8–20 (2010).

DOI: 10.1038/NCLIMATE2574

7. Robin, G. d. . Ice cores and climatic changes. *Phil .Trans. R. Soc. London B* **280,** 143–168 (1977).

8. Parrenin, F. *et al.* The EDC3 chronology for the EPICA Dome C ice core. *Clim. Past* 485–497 (2007).

9. Stenni, B. *et al.* Expression of the bipolar see-saw in Antarctic climate records during the last deglaciation. *Nat. Geosci.* **4,** 46–49 (2011).

10. Jouzel, J. *et al.* Magnitude of isotope/temperature scaling for interpretation of central Antarctic ice cores. *J. Geophys. Res.* **108,** (2003).

11. Blunier, T., Schwander, J., Chappellaz, J., Parrenin, F. & Barnola, J. M. What was the surface temperature in central Antarctica during the last glacial maximum? *Earth Planet. Sci. Lett.* **218,** 379–388 (2004).

12. Uemura, R., Masson-Delmotte, V., Jouzel, J., Landais, A., Motoyama, H., Stenni, B. Ranges of moisture-source temperature estimated from Antarctic ice cores stable isotope records over glacial-interglacial cycles. *Clim. Past* **8,** 1109–1125 (2012).

13. Morgan, V. *et al.* Relative timing of deglacial climate events in Antarctica and Greenland. *Science* **297,** 1862–1864 (2002).

14. Pedro, J. B. *et al.* The last deglaciation: timing the bipolar seesaw. *Clim. Past* **7,** 671–683 (2011).

15. Van Ommen, T. D. & Morgan, V. Calibrating the ice core paleothermometer using seasonality. *J. Geophys. Res.* **102,** (1997).

16. Van Ommen, T. D., Morgan, V. & Curran, M. A. Deglacial and Holocene changes in accumulation at Law Dome, East Antarctica. *Ann. Glaciol.* **39,** 359–365 (2004).

17. WAIS Divide Project Members. Onset of deglacial warming in West Antarctica driven by local orbital forcing. *Nature* **500,** 440–444 (2013).

18. Buizert, C. *et al.* The WAIS-Divide deep ice core WD2014 chronology - part 2: Methane synchronization (68-31 ka BP) and the gas age-ice age difference. *Clim. Past Discuss.* **10,** 3537–3584 (2014).

19. Cuffey, K. M., Clow, G. D., Alley, R. B., Stuiver, M. & Waddington, E. D., Saltus, R. W. Large arctic temperature change at the Wisconsin-Holocene glacial transition. *Science* **270,** 455–458 (1995).

20. Cuffey, K. M. & Clow, G. D. Temperature, accumulation, and ice sheet elevation in central Greenland through the last deglacial transition. *J. Geophys. Res.* **102,** 26383–26396 (1997).

21. Dahl-Jensen, D. *et al.* Past temperatures directly from the Greenland ice sheet. *Science* **282,** 268–271 (1998).